Developmental Cell, Vol. 4, 497–508, April, 2003, Copyright ©2003 by Cell Press

H2AX Is Required for Chromatin Remodeling and Inactivation of Sex Chromosomes in Male Mouse Meiosis

Oscar Fernandez-Capetillo,[1] Shantha K. Mahadevaiah,[2] Arkady Celeste,[1] Peter J. Romanienko,[3] R. Daniel Camerini-Otero,[3] William M. Bonner,[4] Katia Manova,[5] Paul Burgoyne,[2] and André Nussenzweig[1,*]

[1]Experimental Immunology Branch
National Cancer Institute
National Institutes of Health
Bethesda, Maryland 20892

[2]Division of Developmental Genetics
National Institute for Medical Research
Mill Hill
London NW7 1AA
United Kingdom

[3]Genetics and Biochemistry Branch
National Institute of Diabetes and Digestive and Kidney Diseases

[4]Laboratory of Molecular Pharmacology
National Cancer Institute
National Institutes of Health
Bethesda, Maryland 20892

[5]Molecular Cytology Core Facility and Molecular Biology Program
Memorial Sloan-Kettering Cancer Center
New York, New York 10021

Summary

During meiotic prophase in male mammals, the X and Y chromosomes condense to form a macrochromatin body, termed the sex, or XY, body, within which X- and Y-linked genes are transcriptionally repressed. The molecular basis and biological function of both sex body formation and meiotic sex chromosome inactivation (MSCI) are unknown. A phosphorylated form of H2AX, a histone H2A variant implicated in DNA repair, accumulates in the sex body in a manner independent of meiotic recombination-associated double-strand breaks. Here we show that the X and Y chromosomes of histone H2AX-deficient spermatocytes fail to condense to form a sex body, do not initiate MSCI, and exhibit severe defects in meiotic pairing. Moreover, other sex body proteins, including macroH2A1.2 and XMR, do not preferentially localize with the sex chromosomes in the absence of H2AX. Thus, H2AX is required for the chromatin remodeling and associated silencing in male meiosis.

Introduction

In the late 19th century, Lenhossek observed a densely staining body in the nuclei of mammalian spermatocytes in meiotic prophase I (Lenhossek, 1898). Subsequently, this nuclear structure was identified as the highly condensed X-Y chromosome pair (Painter, 1924). Originally called the sex vesicle, it is now termed the sex, or XY, body, since it is not membrane bound (Solari, 1974). Unlike the autosomes, which synapse along their entire lengths, the heteromorphic X-Y pair (gonosomes) only achieves limited synapsis. This is mediated by the "pseudoautosomal" region (PAR), a region of shared DNA sequence homology, spanning approximately 700 kb in laboratory mice (Perry et al., 2001). The condensation of the X and Y chromatin begins at the late zygotene stage and, by mid pachytene (the stage in which homologous chromosome pairs are completely aligned), the sex chromatin forms a microscopically distinct spherical structure near the nuclear periphery (Solari, 1974). Although condensation does not begin until zygotene, the X and Y chromosomes are already distinguished from the autosomes prior to meiotic entry, as evidenced by the fact that they replicate their DNA later than the autosomes at the preleptotene S phase (Odartchenko and Pavillard, 1970).

By the time the sex body has formed, the condensed X and Y chromatin is transcriptionally inactive, as evidenced by the lack of incorporation of uridine and exclusion of RNA polymerase II from the sex body (Monesi, 1965; Turner et al., 2000; Wiltshire et al., 1998). However, the PAR region of the X and Y chromosomes probably escapes this transcriptional inactivation (Raman and Das, 1991). In contrast to the non-PAR regions of the gonosomes, the autosomes at this stage are in a decondensed, transcriptionally active and nuclease-accessible configuration (Solari, 1974; Wiltshire et al., 1998). The transcriptional repression associated with sex body formation, termed meiotic sex chromosome inactivation (MSCI), is reflected in a marked downregulation of several X- and Y-linked transcripts (Mahadevaiah et al., 1998; McCarrey and Dilworth, 1992; McKee and Handel, 1993; Odorisio et al., 1996; Singer-Sam et al., 1990). Concomitant with this transcriptional silencing, autosomal "backups" of several X-linked genes are activated in order to maintain essential metabolic functions in the absence of their silenced counterparts (McKee and Handel, 1993).

The condensation of the gonosomes to form a sex body is likely mediated by the association of specific proteins to the chromatin and by differential histone modifications, such as phosphorylation, ubiquitinization, methylation, or acetylation (Baarends et al., 1999; Strahl and Allis, 2000; Turner et al., 2000). Some proteins, such as the histones macroH2A1.2 (Hoyer-Fender et al., 2000) and H2AX (in its phosphorylated form, γ-H2AX) (Mahadevaiah et al., 2001), together with the protein XMR (Escalier and Garchon, 2000), localize preferentially to the gonosomal chromatin in late zygotene/early pachytene spermatocytes, during the initial stages of gonosomal condensation. These proteins are thus candidates for playing a role in initiating the remodeling of gonosomal chromatin. By late pachytene/early diplotene, the heterochromatin protein HP1β (M31), in addition to its localization to pericentromeric heterochromatin, is concentrated in the sex body (Motzkus et al., 1999; Turner et al., 2001), as befits a heterochromatin domain.

*Correspondence: andre_nussenzweig@nih.gov

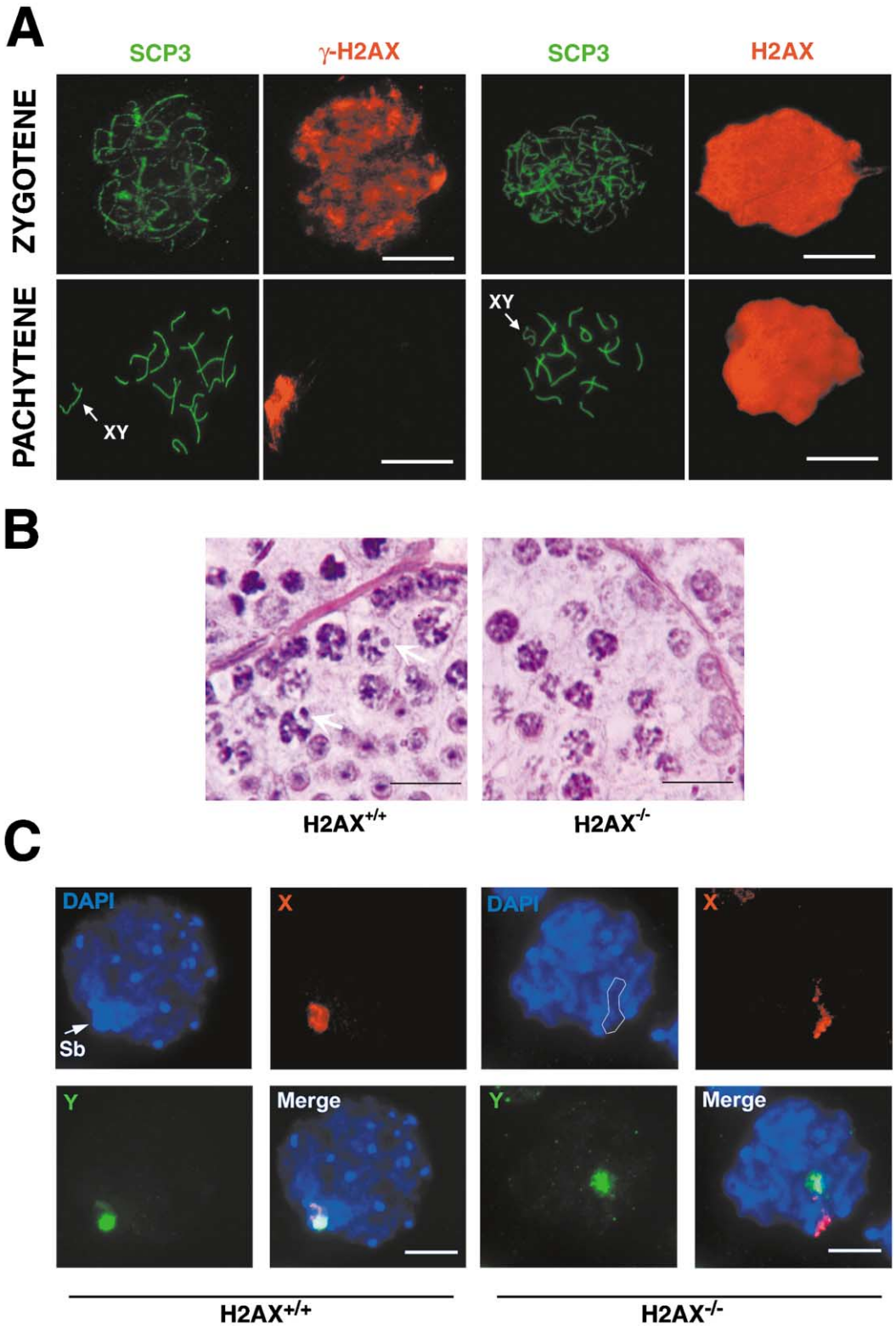

Figure 1. Absence of Sex Body in H2AX-Deficient Spermatocytes

(A) Distribution of phosphorylated (γ-H2AX) and unphosphorylated (H2AX) H2AX in zygotene and pachytene stage wild-type spermatocytes. Cells were immunostained with either γ-H2AX (red)/SCP3 (green) (left panels) or H2AX (red)/SCP3 (green) (right panels). In pachytene stage cells, γ-H2AX is concentrated in the gonosomal domain, whereas unphosphorylated H2AX is depleted from this domain (indicated by the arrow). The scale bar represents 10 μm.

(B) Histological analysis of *H2AX*$^{+/+}$ and *H2AX*$^{-/-}$ seminiferous tubules at stages V–VI of spermatogenesis (PAS staining). Whereas the sex

Besides these proteins with a putative role in the condensation and heterochromatinization process, there is an increasing catalog of proteins that have been shown to accumulate in the gonosomal chromatin domain (Bauer et al., 1998; Calenda et al., 1994; Hoyer-Fender et al., 2000; Kralewski et al., 1997; Motzkus et al., 1999; O'Carroll et al., 2000; Parraga and del Mazo, 2000; Richler et al., 2000; Smith and Benavente, 1992; Smith and Benavente, 1995; Turner et al., 2000). Some of these factors may redistribute to gonosomal chromatin in response to the presence of asynapsed chromatin axes and may thus either be components of the meiotic surveillance machinery that monitors chromosome synapsis or could be involved in masking the non-PAR axes from the pachytene checkpoint (Turner et al., 2000).

The phosphorylation of H2AX to form γ-H2AX is one of the earliest cellular responses to the formation of DNA double-strand breaks (DSBs) (Redon et al., 2002). The use of specific antibodies against γ-H2AX has shown that meiotic recombination in mice is initiated by programmed DSBs catalyzed by the transesterase SPO11 (Keeney, 2001) during leptotene (Baudat et al., 2000; Mahadevaiah et al., 2001; Romanienko and Camerini-Otero, 2000). γ-H2AX forms at sites of SPO11-mediated DSBs, and, subsequently, the loss of γ-H2AX staining occurs in conjunction with synapsis (Mahadevaiah et al., 2001). However, the location of γ-H2AX to the gonosomal chromatin domain in late zygotene is independent of SPO11-mediated DSBs (Mahadevaiah et al., 2001). Furthermore, analysis of spermatocytes from *SPO11*$^{-/-}$*ATM*$^{-/-}$ as well as SCID mice has revealed that the ATM and DNA-PK kinases are not required for γ-H2AX formation on gonosomal chromatin (P.J.R. and R.D.C.-O., submitted). The role of this SPO11-independent γ-H2AX that decorates the sex chromosomes is unclear, although it has been proposed that H2AX phosphorylation may be involved in gonosomal chromatin reorganization in the sex body (Mahadevaiah et al., 2001).

We have previously shown that H2AX-deficient male, but not female, mice are infertile and have increased levels of X-Y asynapsis (Celeste et al., 2002). Here we show that *H2AX*$^{-/-}$ mice do not form a sex body and fail to undergo MSCI. Moreover, apoptotic elimination of *H2AX*$^{-/-}$ spermatocytes at the pachytene stage occurs via a p53-independent apoptotic pathway. Thus, H2AX is essential for the condensation and silencing of the male sex chromosomes.

Results

H2AX Is a Widespread Component of Spermatocyte Chromatin

Although γ-H2AX has previously been localized in spermatocytes, the distribution of unphosphorylated H2AX has not been examined. We therefore began by comparing the localization of these two forms in zygotene and pachytene spermatocytes (Figure 1A). As previously shown, early zygotene spermatocytes exhibit a SPO11-dependent γ-H2AX immunostaining associated with the chromatin of forming synaptonemal complexes (Mahadevaiah et al., 2001). Immediately after synapsis γ-H2AX disappears from autosomal chromatin, but an increasingly intense signal develops over the gonosomal chromatin, such that, by pachytene, only this gonosomal signal remains (Figure 1A). This gonosomal localization of γ-H2AX has been shown to be SPO11 independent (Mahadevaiah et al., 2001). Using immunofluorescence staining with an antibody specific to unphosphorylated H2AX (Bassing et al., 2002), we found that, in contrast to γ-H2AX, H2AX is widely and uniformly distributed throughout the chromatin at zygotene. This is consistent with the requirement for H2AX to be available for phosphorylation at the sites of DSBs that occur throughout the chromatin. There is then a very noticeable depletion of the unphosphorylated form in the gonosomal domain, so that, at pachytene, the X-Y pair lie in an H2AX-depleted "pocket" (Figure 1A). This undoubtedly reflects the phosphorylation of the majority of H2AX to form γ-H2AX in this location. Importantly, staining for both γ-H2AX (Celeste et al., 2002) and H2AX (see Supplemental Figure S1 at http://www.developmentalcell.com/cgi/content/full/4/4/497/DC1) disappears in *H2AX*$^{-/-}$ spermatocytes, confirming the specificity of the antibodies. Thus, SPO11-independent γ-H2AX staining of gonosomal chromatin is due to a massive phosphorylation of H2AX, rather than a preferential increase in the local concentration of H2AX.

Absence of Sex Body in *H2AX*$^{-/-}$ Mice

In sections of seminiferous tubules from wild-type mice, the presence of a sex body could already be discerned in pachytene spermatocytes by about stage V of the spermatogenic cycle (Figure 1B). Although *H2AX*$^{-/-}$ spermatocytes are still present in stage V/VI seminiferous tubules, sex bodies were conspicuously absent (Figure 1B and Table 1). Moreover, analysis of *H2AX*$^{-/-}$*p53*$^{-/-}$ testes revealed that loss of p53 did not rescue either the meiotic arrest or the formation of the sex body (Table 1; see Supplemental Figure S2 at http://www.developmentalcell.com/cgi/content/full/4/4/497/DC1). To examine the condensation status of the sex chromosomes in *H2AX*$^{+/+}$ and *H2AX*$^{-/-}$ spermatocytes, we hybridized surface-spread spermatocytes with painting probes to identify X and Y chromosomes. In many of the *H2AX*$^{+/+}$ spermatocytes, the X-Y pair was found in a highly heterochromatic DAPI-rich region localized at the nuclear periphery (Figure 1C). By contrast, the sex chromosomes appeared to be randomly spread within the *H2AX*$^{-/-}$ spermatocyte nuclei. Although the majority of the

body is prominent in wild-type pachytene cells at this stage (white arrows), no morphological manifestation of the sex body is observable in the *H2AX*$^{-/-}$ pachytene cells. The scale bar represents 40 μm.

(C) FISH labeling of *H2AX*$^{+/+}$ and *H2AX*$^{-/-}$ spermatocytes with X (red) and Y (green) chromosome-specific probes, counterstained with DAPI (blue). In wild-type pachytene spermatocytes, the condensed X and Y chromosomes are located in the heterochromatic sex body (Sb). In *H2AX*$^{-/-}$ spermatocytes the X and Y are less condensed and are located in a region of euchromatin (outlined in the DAPI panel). The scale bar represents 10 μm.

Table 1. Analysis of Sex Body Formation in H2AX Wild-Type and Mutant Mice

Genotype	Number of Cells Analyzed	Cells Presenting a Sex Body	Type of Assay
H2AX$^{+/+}$	480	176	Histological examination (PAS)[a,b]
H2AX$^{-/-}$	325	0	
H2AX$^{+/+}$	30	19	X-Y chromosome painting plus DAPI[a]
H2AX$^{-/-}$	100	0	
H2AX$^{+/+}$	26	25	H1t immunostaining plus DAPI
H2AX$^{-/-}$	26	0	
H2AX$^{+/+}$	75	75	H1t immunostaining plus Xmr
H2AX$^{-/-}$	78	0	

[a] No staging marker was present in the X-Y chromosome painting or in the histological analysis (PAS).
[b] Zero out of 450 *H2AX*$^{-/-}$p53$^{-/-}$ pachytene cells showed a sex body by histological analysis (PAS).

H2AX$^{-/-}$ spermatocytes were arrested in pachytene, as determined by staining with antibodies specific to synaptonemal complex proteins (data not shown) (Celeste et al., 2002), we did not find a single highly condensed DAPI-rich nuclear domain where the X and Y chromosomes resided (n = 200) (Figure 1C and Table 1).

Morphologically distinct sex bodies do not appear until mid/late pachytene in wild-type mice. To determine whether *H2AX*$^{-/-}$ cells reached this stage, we immunostained squash preparations with an antibody against H1t, a testis-specific linker histone that is transcribed from the mid and late pachytene through the spermatid stages (Drabent et al., 1996). H1t-positive spermatocytes were also present in *H2AX*$^{-/-}$ testes (see Supplemental Figure S3 at http://www.developmentalcell.com/cgi/content/full/4/4/497/DC1). Of 26 H1t-positive *H2AX*$^{-/-}$ spermatocytes scored under the microscope while viewing the DAPI signal alone, none possessed a sex body, as assessed by DAPI staining, whereas 25 out of 26 H1t-positive *H2AX*$^{+/+}$ spermatocytes had an unambiguous sex body (Table 1). Taken together, these data demonstrate that loss of H2AX is associated with the absence of a sex body.

Sex Body-Associated Proteins Do Not Concentrate on the Gonosomal Chromatin Domain in *H2AX*$^{-/-}$ Spermatocytes

The preferential association of macroH2A1.2 and XMR with gonosomal chromatin in late zygotene/early pachytene spermatocytes from normal males makes them candidates for a role in initiating gonosomal condensation (Calenda et al., 1994; Escalier and Garchon, 2000; Hoyer-Fender et al., 2000; Kralewski et al., 1997; Mahadevaiah et al., 2001; Motzkus et al., 1999). To determine whether the concentration of these proteins in gonosomal chromatin is affected in *H2AX*$^{-/-}$ spermatocytes, we used immunostaining to examine the distribution of these proteins. In spread *H2AX*$^{+/+}$ spermatocytes, macroH2A1.2 colocalized with intense γ-H2AX staining, and XMR was concentrated over the asynaped X and Y axes, consistent with previous results (Figures 2A and 2B). By contrast, no discrete macroH2A1.2 or XMR staining was found in *H2AX*$^{-/-}$ spermatocytes (Figures 2A and 2B). XMR localization was further examined in squash preparations in combination with H1t (to identify the mid pachytene through diplotene stages) (Figure 2C). In controls, there was the expected whole nuclear staining at leptotene and zygotene, with an accumulation on gonosomal chromatin in late zygotene/early pachytene, and then restriction of XMR to the sex body in mid pachytene through diplotene. All H1t positive pachytene/diplotene control cells (n = 75) examined showed an XMR-positive sex body (Table 1). In contrast, although *H2AX*$^{-/-}$ spermatocytes showed whole nuclear XMR staining in leptotene and zygotene, there was no preferential localization to the gonosomal chromatin at any stage, including in H1t-positive cells (n = 78) (Figure 2C and Table 1). Thus, the deposition of XMR and macroH2A1.2 on gonosomal chromatin is disrupted in *H2AX*$^{-/-}$ mice. Since XMR and macroH2A1.2 normally concentrate on the sex chromosomes, before or coincident with condensation, it is likely that H2AX is essential for the initiation of sex body formation.

Failure to Undergo Meiotic Sex Chromosome Inactivation in *H2AX*$^{-/-}$ Mice

The X-inactive transcript (*Xist*) is essential for X inactivation in female mammals and for the preferential localization of macroH2A1.2 on the inactive X chromosome (Csankovszki et al., 1999). It has been postulated that MSCI is also initiated by *Xist* RNA (Ayoub et al., 1997), but recent analyses of male mice with targeted disruptions of *Xist* suggest that MSCI is largely, if not completely, *Xist* independent (McCarrey et al., 2002; Turner et al., 2002). Nevertheless, it is generally accepted that the condensation of the gonosomal chromatin to form the sex body (a feature retained in *Xist* mutant mice) contributes to MSCI, perhaps by leading to the exclusion of proteins involved in transcription, such as RNA polymerase II (pol II) (Richler et al., 1994). We therefore asked whether the failure of gonosomal condensation in *H2AX*$^{-/-}$ males resulted in a failure of MSCI.

We first examined the distribution of RNA pol II by immunostaining. In control cells, RNA pol II was excluded from the sex body (Richler et al., 1994; Turner et al., 2000), which exhibited intense γ-H2AX staining (Figure 3A). By contrast, we observed a uniform distribution of RNA pol II throughout the nucleus of *H2AX*$^{-/-}$ spermatocytes (Figure 3A). This included the region where the X-Y pair was localized, as determined by immunostaining for BRCA1 (Figure 3A), which marks the sex chromosome axes during pachytene (Scully et al., 1997).

To further evaluate the impact of H2AX deficiency on MSCI, we performed microarray-based analysis of nearly 10,000 murine genes from two independent preparations of *H2AX*$^{+/+}$ and *H2AX*$^{-/-}$ spermatocytes. In an attempt to minimize differences in spermatogenic cell

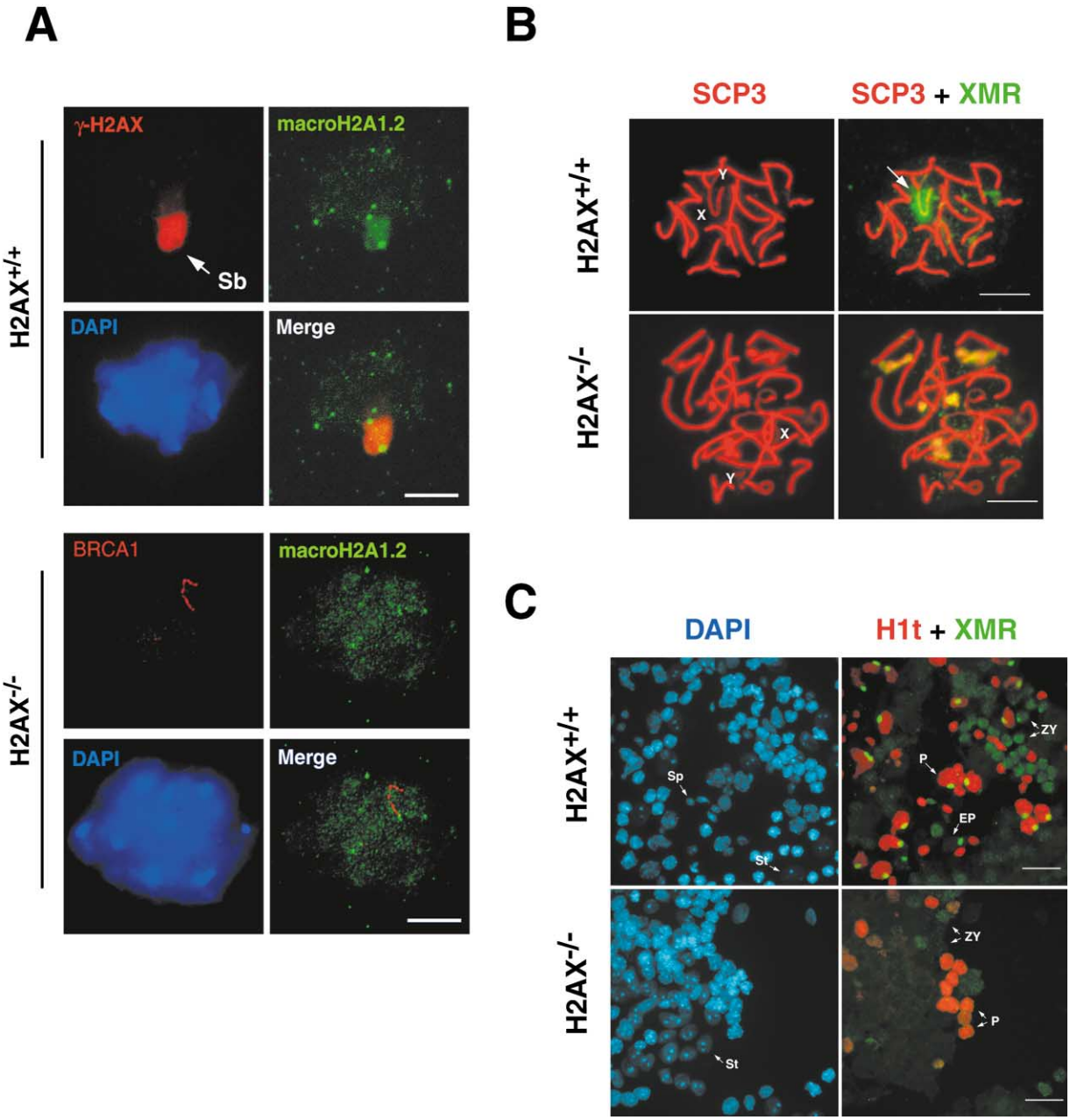

Figure 2. H2AX Is Required for the Concentration of Sex Body-Associated Factors to Gonosomal Chromatin

(A) γ-H2AX (red)/macroH2A1.2 (green) and BRCA1 (red)/macroH2A1.2 (green) immunostaining of spread *H2AX*$^{+/+}$ and *H2AX*$^{-/-}$ pachytene spermatocytes, respectively, counterstained with DAPI (blue). In *H2AX*$^{+/+}$ spermatocytes macroH2A1.2 and γ-H2AX colocalize in the sex body (Sb). In *H2AX*$^{-/-}$ pachytene spermatocytes there was no localization of macroH2A1.2 to the gonosomal domain (located by BRCA1 staining of the X and Y chromosome axes). The scale bar represents 10 μm.

(B) SCP3 (red)/XMR (green) immunostaining of spread *H2AX*$^{+/+}$ and *H2AX*$^{-/-}$ pachytene spermatocytes. The XLR antibody (which detects XMR) stains chromatin associated with asynapsed axes. In the wild-type early pachytene cell, the XMR staining is concentrated over the chromatin associated with the asynapsed non-PAR axes of the X-Y bivalent (white arrow). In *H2AX*$^{-/-}$ spermatocytes there was no accumulation of XMR staining associated with the gonosomal axes (indicated). Some nonspecific XMR staining of nucleoli is observed. The scale bar represents 10 μm.

(C) H1t (red)/XMR (green) immunostaining in squash preparations of *H2AX*$^{+/+}$ and *H2AX*$^{-/-}$ testes, counterstained with DAPI (blue). The wild-type image shows the expected pattern of XMR staining, with whole nuclear staining at zygotene (Zy), much reduced whole nuclear staining, but clear sex body staining, in H1t-negative early pachytene cells (EP), and then staining restricted to the sex body in the H1t-positive mid pachytene (P) and late pachytene spermatocytes (the other H1t-positive cells are round and condensing spermatids). In contrast, although *H2AX*$^{-/-}$ spermatocytes show the whole nuclear staining pattern in zygotene, XMR never concentrates to form a clear sex body domain. The scale bar represents 50 μm.

A

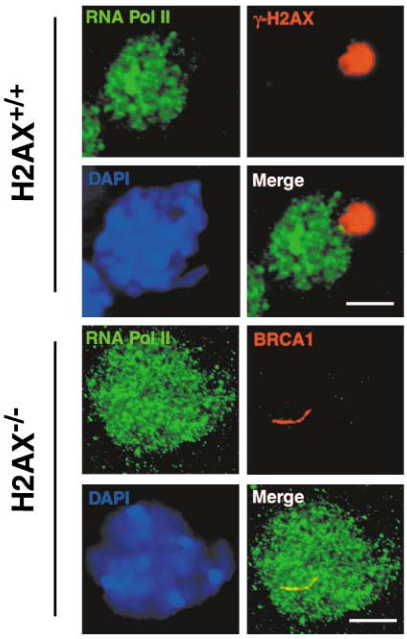

B

Transcript	Gene	Chromosome	Ratio
Rgs2	regulator of G-protein signaling 2	1	4.9366
Cstb	cystatin B	10	3.9697
Gsta4	glutathione S-transferase, alpha 4	9	3.7747
Rbbp7	retinoblastoma binding protein 7	X	3.6439
Cycs	cytochrome c, somatic	6	3.5699
Syngr2	synaptogyrin 2	11	3.4756
Gstm1	glutathione S-transferase, mu 1	3	3.3483
Cst9	cystatin 9	2	3.2157
Zfp364	zinc finger protein 364	3	3.1889
Meox1	mesenchyme homeobox 1	11	3.094
Enah	enabled homolog (Drosophila)	1	3.0743
Thrsp	thyroid hormone responsive SPOT14 homolog (Rattus)	7	3.0125
Aldh1a7	aldehyde dehydrogenase family 1, subfamily A7	19	2.945
Cul4b	cullin 4B	X	2.864
Kitl	kit ligand	10	2.824
Hmgb3	high mobility group box 3	X	2.798
Rex3	reduced expression 3	X	2.776
Fgfrp	fibroblast growth factor regulated protein	6	2.698
Eif2S3y	eukaryotic translation initiation factor 2, subunit 3, ...	Y	2.558
Idb1	inhibitor of DNA binding 1	2	2.521
Cpe	carboxypeptidase E	8	2.468
Lamp2	lysosomal membrane glycoprotein 2	X	2.354
Bhmt	betaine-homocysteine methyltransferase	18	2.321
Cd81	CD 81 antigen	7	2.198
AU023707	AU023707	X	2.098

C

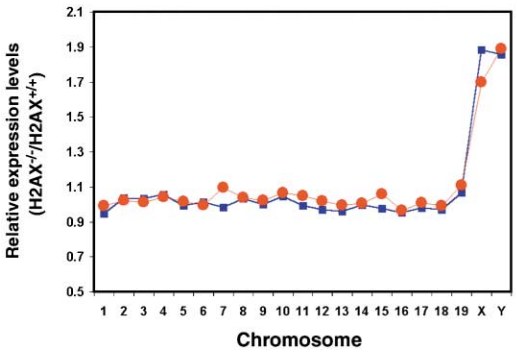

D

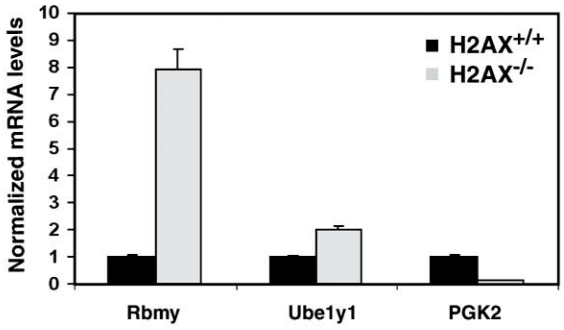

Figure 3. Impaired MSCI in H2AX-Deficient Spermatocytes

(A) γ-H2AX (red)/RNA polymerase II (green) and BRCA1 (red)/RNA polymerase II (green) immunostaining of spread *H2AX*$^{+/+}$ and *H2AX*$^{-/-}$ pachytene spermatocytes, respectively, counterstained with DAPI (blue). RNA pol II is excluded from the sex body (γ-H2AX-positive domain) in *H2AX*$^{+/+}$ cells but is uniformly distributed over the entire nucleus in *H2AX*$^{-/-}$ cells, including the gonosomal domain (located by BRCA1 staining of the X and Y axes). The scale bar represents 10 μm.

(B) Microarray analysis of gene expression in *H2AX*$^{+/+}$ and *H2AX*$^{-/-}$ testes. Total testis RNA was either Cy5- or Cy3-labeled and hybridized against a glass microarray containing 9656 murine cDNAs. The table lists the 25 cDNAs with the highest *H2AX*$^{-/-}$/*H2AX*$^{+/+}$ intensity ratios, averaged between two experiments with 16.5- and 18.5-day-old preparations, respectively. cDNAs from X- and Y-linked genes (highlighted in blue or orange, respectively) are overrepresented.

(C) Relative (*H2AX*$^{-/-}$/*H2AX*$^{+/+}$) levels of expression on a chromosome by chromosome basis, as determined by microarray analysis. There is a statistically significant upregulation of X- and Y-linked genes (Student's t test, $p < 0.01$) in both 16.5 (red, filled circles)- and 18.5 (blue, filled squares)-day-old preparations.

(D) Quantitative RT-PCR analysis of *H2AX*$^{+/+}$ and *H2AX*$^{-/-}$ testis RNA for Y chromosome genes known to be targets of MSCI. *Rbmy* and *Ube1y1* transcript levels (normalized against β-actin) are increased in *H2AX*$^{-/-}$ cells (7.89-fold and 2.1-fold, respectively). Although transcripts for the autosomal backup *Pgk-2* are easily detected in *H2AX*$^{+/+}$ cells, they are almost undetectable in *H2AX*$^{-/-}$ spermatocytes (7.14-fold reduction).

populations between H2AX$^{-/-}$ testes and those of controls, we obtained RNA from *H2AX*$^{+/+}$ and *H2AX*$^{-/-}$ littermates at 16.5 or 18.5 days after birth, when the most advanced stage is mid or late pachytene, respectively (Nebel et al., 1961). For the data analysis, we arranged the genes on the basis of the maximum differences in expression level. It was immediately clear that a disproportionate number of X-linked genes were overexpressed in *H2AX*$^{-/-}$ spermatocytes (Figure 3B). When we compared the expression level of genes from individual

chromosomes, we found that the majority of autosomal genes were expressed similarly in the *H2AX*$^{+/+}$ and *H2AX*$^{-/-}$ spermatocytes (the average ratio was not significantly different from 1; Student's t test) (Figure 3C). In contrast, the average levels of X-linked genes and the three Y-linked genes *Eif2s3y*, *Dby*, and *Smcy*, represented on the microarray, were increased in H2AX-deficient cells. The average ratio for X- and Y-linked genes was 1.9, which was significantly different from the average expression level for autosomal genes (Student's t test, $p = 0.001$) (Figure 3C). We conclude that a disproportionate number of genes residing on the sex chromosomes are overexpressed in *H2AX*$^{-/-}$ spermatocytes.

To determine whether specific Y genes that were previously reported to be targets of MSCI were affected by the absence of H2AX, we compared the expression of *Ube1y1* (Odorisio et al., 1996) and *Rbmy* (Mahadevaiah et al., 1998; Turner et al., 2000) (both of which were not represented on the microarray) in 18.5-day-old *H2AX*$^{+/+}$ and *H2AX*$^{-/-}$ littermates by quantitative real-time RT-PCR (Figure 3D). In *H2AX*$^{-/-}$ testes, the Y-linked *Ube1y1* and *Rbmy* genes were overexpressed by 2- and 8-fold, respectively. The autosomal gene PGK2 acts as a backup for the X-linked counterpart PGK1, and it is presumed that PGK activity is essential for spermatocyte survival (McKee and Handel, 1993). In support of the idea that overexpression of X- and Y-linked genes is related to a failure in the process of MSCI, the expression of *Pgk-2* was significantly lower in the H2AX-deficient cells (Figure 3D). We therefore conclude that MSCI is impaired in *H2AX*$^{-/-}$ mice.

To determine whether the absence of MSCI resulted in the inappropriate expression of sex-linked genes specifically during pachytene, we examined the distribution of RBMY in *H2AX*$^{+/+}$ and *H2AX*$^{-/-}$ spermatocytes by immunostaining. RBMY is a nuclear splicing protein, which, in normal males, falls to an undetectable level by mid pachytene (Mahadevaiah et al., 1998; Turner et al., 2002). However, aberrant expression of RBMY has been observed in XYY spermatocytes with sex body anomalies (Turner, 2000). RBMY immunostaining was performed on squash preparations, and mid/late pachytene cells were identified on the basis of immunostaining for HP1β, which exhibits intense staining of centromeric heterochromatin at this stage (Turner et al., 2001). Whereas wild-type mid/late pachytene cells were negative for RBMY, most of the *H2AX*$^{-/-}$ cells with clear HP1β autosomal centromere staining were intensely stained for RBMY (see Supplemental Figure S4 at http://www.developmentalcell.com/cgi/content/full/4/4/497/DC1).

More detailed analysis of RBMY expression was carried out on spread spermatocytes staged by SCP3 staining of the synaptonemal complexes and CREST staining of the centromeres and by measuring the total RBMY fluorescence signal in the nucleus at different stages. RBMY levels decreased steadily from preleptotene to pachytene in wild-type spermatocytes; in *H2AX*$^{-/-}$ spermatocytes, RBMY levels again decreased from preleptotene through zygotene, but levels then increased dramatically during pachytene (Figures 4A and 4B). Thus, consistent with the observed transcript levels, this Y-linked protein is aberrantly expressed in *H2AX*$^{-/-}$ pachytene stage spermatocytes. Moreover, by analyzing pachytene stage cells in situ, we have ruled out the possibility that the increased *Rbmy* transcript levels seen by RTPCR in *H2AX*$^{-/-}$ testes were due to a difference in the relative frequencies of spermatocyte subpopulations compared with the controls.

X-Y Synapsis Defects in *H2AX*$^{-/-}$ Mice

Pairing of X and Y chromosomes at the pseudoautosomal region is essential for male fertility (Burgoyne et al., 1992a; Miklos, 1974). Some degree of X-Y asynapsis has been observed in *H2AX*$^{-/-}$ males, but almost 65% of the pachytene cells from 2-month-old mice achieve normal synapsis (Celeste et al., 2002). Here we determined the frequency of X-Y asynapsis by immunostaining for the synaptonemal complex proteins SCP3/SCP1 in 16-day-old *H2AX*$^{+/+}$ and *H2AX*$^{-/-}$ spermatocytes. In striking contrast to the 16-day-old sibling controls, which showed 1.8% X-Y asynapsis ($n = 55$), 88% of *H2AX*$^{-/-}$ pachytene stage cells from preweanlings exhibited X and Y chromosomes that failed to synapse ($n = 50$). In 32% of the *H2AX*$^{-/-}$ cells, the X chromosome also showed an apparent association with autosomes. Thus, there appears to be a particularly high level of X-Y asynapsis in young *H2AX*$^{-/-}$ mice. Although it remains unclear why spermatocytes from adult *H2AX* mutant testes exhibit lower levels of X-Y asynapsis than those from prepubertal males, this may indicate that cells with asynapsed X and Y chromosomes are selectively removed at an unusually early stage.

Normal Localization of Rad51 in Spread *H2AX*$^{-/-}$ Spermatocyte Nuclei

Since H2AX is implicated in DNA repair (Bassing et al., 2002; Celeste et al., 2002; Downs et al., 2000) and is essential for the recruitment of several DNA repair factors (excluding RAD51) into irradiation-induced foci (Bassing et al., 2002; Celeste et al., 2002), it is possible that meiotic DSBs are inefficiently processed in the absence of H2AX. To monitor the formation and resolution of DSBs in *H2AX*$^{-/-}$ mice, we examined the distribution of RAD51, which forms foci at sites of meiotic DSBs. The initiation of DSBs was normal in *H2AX*$^{-/-}$ males, as judged from the appearance of RAD51 foci in zygotene (Figure 5). Unlike γ-H2AX, which saturates the sex body in pachytene spermatocytes independently of SPO11-initiated DSBs (Mahadevaiah et al., 2001), a few SPO11-dependent RAD51 foci persisted into pachytene, mainly on the asynapsed X chromosomes (Mahadevaiah et al., 2001; Moens et al., 1997), in both *H2AX*$^{+/+}$ and *H2AX*$^{-/-}$ mice (Figure 5). Although the precise relationship between the timing of RAD51 resolution and DSB repair in mouse spermatocytes is unclear, it is presumed that DSBs are processed by the time RAD51 foci disappear (Moens et al., 1997) (Figure 5). In *H2AX*$^{-/-}$ spermatocytes, RAD51 foci disappeared on schedule after synapsis (Figure 5), indicating that DSBs are processed in *H2AX*$^{-/-}$ spermatocytes.

Discussion

The present study shows that the pachytene arrest that causes the male-specific sterility in *H2AX*$^{-/-}$ mice is associated with the complete absence of the macrochromatin sex body, a global failure to inactivate gonosomal

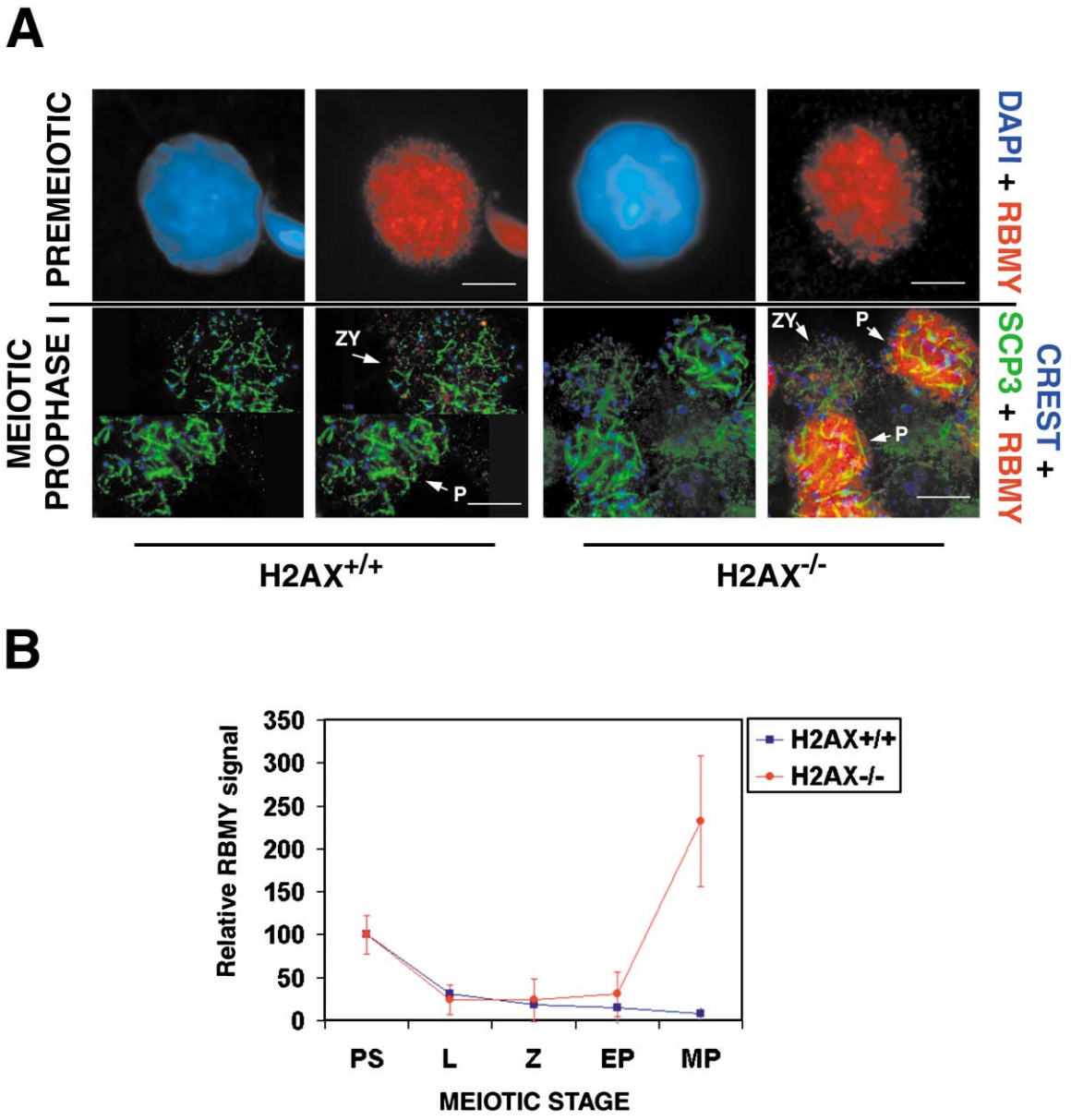

Figure 4. Altered Expression Pattern of RBMY Protein during Spermatogenesis in H2AX-Deficient Mice

(A) SCP3 (green)/RBMY (red) immunostaining of spread *H2AX*$^{+/+}$ and *H2AX*$^{-/-}$ testicular cells, counterstained with DAPI (blue). CREST human sera was used to stain centromeric regions (blue pseudo-color) in order to help distinguish zygotene (incomplete pairing of centromeres) and pachytene stages (all centromeres paired). In wild-type and mutant cells, RBMY is expressed at high levels in preleptotene stages and is reduced to low levels at zygotene (Zy). However, whereas, in wild-type pachytene cells, RBMY has fallen to undetectable levels, it is strongly expressed in *H2AX*$^{-/-}$ pachytene spermatocytes. The scale bar represents 5 μm in premeiotic panels and 10 μm in meiotic prophase I panels. (B) Analysis of RBMY levels at different meiotic stages. The integrated values of the RBMY immunofluorescent signals, as described in (A), for five nuclei of different meiotic stages, as staged with DAPI/SCP3/CREST staining (PS; preleptotene; L, leptotene; Z, zygotene; EP, early pachytene; MP, mid pachytene).

chromatin, and defects in X-Y synapsis. These meiotic dysfunctions correlate with the kinetics of γ-H2AX accumulation and loss in the gonosomal domain. The marked accumulation of SPO11-independent γ-H2AX throughout the gonosomal chromatin domain occurs at late zygotene (Mahadevaiah et al., 2001), and we show here that this is due to the phosphorylation of the majority of H2AX. This massive phosphorylation of H2AX is coincident with the onset of gonosomal chromatin condensation and X-Y synapsis (Goetz et al., 1984). The phosphorylated isoform subsequently disappears from the gonosomal chromatin precisely when the sex body disperses at the diplotene-metaphase I transition (Mahadevaiah et al., 2001). These observations suggest that the

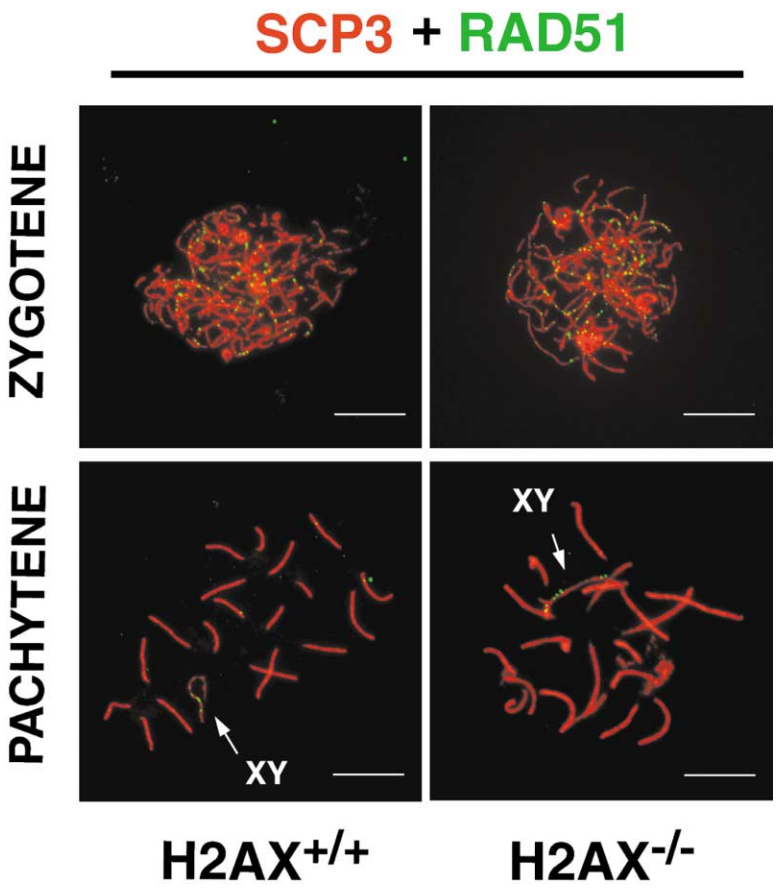

Figure 5. Normal Distribution of RAD51 in H2AX-Deficient Spermatocytes

Merged image of SCP3 (red) and RAD51 (green) in *H2AX*$^{+/+}$ and *H2AX*$^{-/-}$ zygotene and pachytene stage spermatocytes. The arrow shows the X-Y chromosome pair. The scale bar represents 10 μm.

state of H2AX phosphorylation may regulate its ability to affect chromatin remodeling and associated silencing of the male sex chromosomes. According to this model, H2AX phosphorylation would be essential for initiation of heterochromatization in the sex body, and the subsequent dephosphorylation of H2AX would be required for effecting the decrease in sex chromatin condensation at the end of diplotene, ensuring a proper chromosome configuration before metaphase I.

One interesting feature of the sex body-associated H2AX phosphorylation is its independence not only of meiotic recombination-associated DSBs mediated by SPO11 (Mahadevaiah et al., 2001), but also of the ATM and DNA-PK kinases, which are predominantly involved in responding to DSBs (Abraham, 2001; van Gent et al., 2001). Besides ATM and DNA-PK, the only other phosphatidylinositol 3-kinase (PI3K)-like protein kinase that is known to phosphorylate H2AX is ATR (Ward and Chen, 2001). In contrast to ATM, which accumulates on synapsed chromosome axes (Keegan et al., 1996), ATR loads onto chromosomal segments that are not fully synapsed (Keegan et al., 1996; Moens et al., 1999). Similarly, γ-H2AX is associated with unpaired chromosomal segments (Mahadevaiah et al., 2001). Strikingly, the unpaired regions of the X-Y chromosomes exhibit extensive labeling with both anti-ATR and anti-γ-H2AX antibodies (Keegan et al., 1996; Mahadevaiah et al., 2001; Moens et al., 1999). These observations suggest that the constitutive asynapsis of the sex chromosomes is the signal that recruits ATR to chromatin and induces H2AX phosphorylation throughout the sex body. However, the fact that ATR-deficient mice are inviable precludes a formal demonstration of this hypothesis.

The functions of the sex body during meiosis remain unclear. The X-Y pair achieves synapsis via the PAR in late zygotene, when γ-H2AX first appears throughout the gonosomal chromatin domain (Goetz et al., 1984). It has been suggested that the sequestration of the non-PARs in association with MSCI and sex body formation may serve to focus the "homology search" that precedes synapsis onto the PARs (Turner et al., 2000). This proposed function is based on the analysis of X-Y females, which have a remarkably similar phenotype to *H2AX*$^{-/-}$ males. In both models, the absence of MSCI and a sex body is associated with severe defects in X-Y synapsis. We have previously shown that homologous integration of targeting constructs is defective in *H2AX*$^{-/-}$ ES cells, indicating that H2AX is required for efficient homologous recombination (Celeste et al., 2002). If H2AX participated in the presynaptic alignment or in stabilizing strand exchanges between partners, then deficiency in H2AX might most profoundly affect the highly recombinagenic PAR (Rappold, 1993), where the strength of the synaptic contacts could be weaker because of the limited degree of homology. Irrespective of the mechanism, X-Y PAR asynapsis is unlikely to be the sole trigger for the apoptotic elimination of all *H2AX*$^{-/-}$ spermatocytes before late pachytene, since, in other mouse models with X-Y

asynapsis, meiotic arrest is predominantly at the first meiotic metaphase (Burgoyne et al., 1992b).

Another of the proposed functions of this macrochromatin domain is to sequester the asynapsed non-PARs of the X-Y bivalent from the pachytene checkpoint (Jablonka and Lamb, 1988). It has been proposed that incompletely processed DSBs on asynapsed axes are the trigger for the pachytene checkpoint that responds to the presence of asynapsed axes during meiosis from yeast to man (Roeder and Bailis, 2000). The presence of RAD51/DMC1 foci marking unprocessed DSBs on the X non-PAR of normal males, which are retained until late pachytene (Moens et al., 1997; Pittman et al., 1998; Yoshida et al., 1998), emphasizes the need to mask the non-PAR axes. Thus, failure to sequester these DSBs within the macrochromatin body of *H2AX*$^{-/-}$ males could be the trigger, in addition to X-Y PAR asynapsis, that accounts for the meiotic failure in mid/late pachytene. Interestingly, *H2AX*$^{-/-}$ mice show a high degree of X-autosome associations (Celeste et al., 2002), which could reflect the exposed nature of the sex chromosomes in the absence of a sex body. Consistent with other models in which sterility is associated with synaptic abnormalities (Odorisio et al., 1998), our results on *H2AX*$^{-/-}$*p53*$^{-/-}$ mice demonstrate that the DNA damage transducer p53 is not involved in the apoptotic elimination of *H2AX*$^{-/-}$ spermatocytes.

Finally, it is possible that the pachytene arrest in *H2AX*$^{-/-}$ males is a direct consequence of the failure to undergo MSCI. Similar to what has been proposed for female dosage compensation, the reactivation of the X- and Y-linked genes in *H2AX*$^{-/-}$ males in conjunction with the turning on of autosomal backups could also lead to lethality if the increased dosage of these proteins led to metabolic imbalances. However, our transcriptional analysis demonstrates that activation of the autosomal backup *Pgk-2* is much reduced in *H2AX*$^{-/-}$ males that fail to undergo MSCI. If this were true of other autosomal counterparts, pachytene arrest due to metabolic imbalances might be less plausible. It is also possible that the aberrant expression of specific X or Y genes could induce apoptosis if transduction of the pachytene checkpoint signal is triggered by the overexpression of certain sex chromosome-linked genes (Mazeyrat et al., 2001). Nevertheless, our data indicate that the normal activation of autosomal backups is directly related to the silencing of the X chromosome, rather than being a consequence of an intrinsic developmental program.

In normal spermatogenesis, RBMY protein levels fall dramatically as cells progress from preleptotene through leptotene and zygotene. Significantly, the same fall in RBMY levels is seen in the *H2AX*$^{-/-}$ males, and it is not until pachytene that the RBMY levels suddenly increase. These results raise the possibility that there is an earlier phase of transcriptional repression of X and Y genes that is H2AX independent. However, the dramatic increase of RBMY levels in *H2AX*$^{-/-}$ spermatocytes, precisely at the stage in which the sex body is normally formed, suggests a link between the onset of gonosomal chromatin condensation at late zygotene and MSCI.

Although H2AX plays an essential role in sex body formation, we cannot rule out the possibility that H2AX deficiency also leads to other meiotic defects affecting all chromosomes. For example, some unprocessed DSBs might be retained on the autosomes of *H2AX*$^{-/-}$ mice after synapsis. However, the level of autosomal asynapsis in these mice does not appear to be sufficient to account for the complete pachytene failure. Moreover, our finding that RAD51 foci disappear on schedule from the synapsed autosomes in *H2AX*$^{-/-}$ mice, together with the fact that H2AX is essential for male, but not female, fertility, argues against a fundamental role for H2AX in meiotic recombination. Thus, the male-specific defect in *H2AX*$^{-/-}$ mice is more likely to be due to loss of an essential function of H2AX with respect to the heteromorphic sex chromosomes.

Although the condensation of the X and Y chromosomes in meiotic cells was observed eight decades ago (Painter, 1924), the function and molecular basis of sex body formation and the associated MSCI remain an enigma. Progress has been hampered by the failure hitherto to identify gene mutations that specifically interfere with either sex chromosome condensation or inactivation. The present study of males homozygous for a null mutation of the histone H2A variant *H2AX* shows that H2AX plays a crucial role in controlling sex chromosome condensation and transcriptional inactivation, supporting the view that these processes are intimately linked. Future studies will be needed to analyze the role of H2AX in heterochromatinization in DSB-dependent or -independent situations and the specific function of H2AX phosphorylation in these processes.

Experimental Procedures

Histological Analysis of the Testis

PAS (periodic acid-Schiff) staining of Bouin's fixed paraffin sections was performed as described (Prophet, 1994). For the analysis of apoptosis, paraffin sections (8 μm) of 4% paraformaldehyde-fixed testes were processed for the TUNEL reaction, in which biotinylated dUTP was added to DNA ends by terminal transferase, as described (Manova et al., 1998).

Immunofluorescent Staining

Meiotic prophase cell spreads and squashes were prepared and stained essentially as previously described (Mahadevaiah et al., 2001; Romanienko and Camerini-Otero, 2000). However, material for processing at the National Institute for Medical Research was first frozen in liquid nitrogen and transported on dry ice, prior to thawing in RPMI medium. For spreading from frozen material, the hypotonic step had to be omitted. Primary antibodies used for immunofluorescence were rabbit anti-γ-H2AX (1:500), rabbit anti-H2AX (1:3000; kindly provided by R. Scully), mouse anti-BRCA1 (1:5; kindly provided by S. Ganesan), rabbit anti-macro.H2A1.2 (1:50; kindly provided by J. Pehrson), rabbit anti-RNA Polymerase II (1:10, C-21; Santa Cruz Biotechnologies), rabbit anti-SCP3 (1:1000; kindly provided by C. Heyting), guinea pig anti-SCP3 (1:250; kindly provided by R. Benavente), rat anti-HP1β (1:500; kindly provided by P. Singh), rabbit anti-RBMY (1:100; kindly provided by D. Elliott), rabbit anti-histone H1t (kindly provided by P. Moens), mouse monoclonal anti-XLR, which recognizes the meiosis-specific XMR (1:500; kindly provided by H.-J. Garchon), and human CREST serum, which recognizes centromeres (1:5000; kindly provided by W. Earnshaw). Secondary antibodies used were goat anti-rabbit Cy3 (Amersham Pharmacia Biotech), goat anti-rabbit Alexa 488 (Molecular Probes), goat anti-mouse Cy3 (Amersham Pharmacia Biotech), goat anti-mouse Alexa 488 (Molecular Probes), goat anti-rat Alexa 488 (Molecular Probes), and goat anti-human Alexa 647. Secondary antibodies were used at 1:250 or 1:500.

RBMY Quantitation

After image capture, the relative amounts of fluorescence from the anti-RBMY antibody were calculated for each of five cells for each

spermatogenic cell stage, sampled with the softWoRx software of the DeltaVision microscope (Applied Precision, Seattle). An outline around the nucleus was drawn, the integrated intensity within this area was calculated, and then the background fluorescence for an equivalent area was subtracted.

Fluorescent In Situ Hybridization (FISH) Analysis of Meiotic X-Y Chromosomes

Meiotic chromosome spreads were prepared following standard methanol-acetic fixation, and chromosome FISH was performed as described (Liyanage et al., 1996). Spreads were hybridized with chromosome-painting probes generated by DOP-PCR with flow-sorted single X and Y chromosomes (Liyanage et al., 1996).

Microarray Analysis

Twenty micrograms of total RNA isolated from *H2AX*$^{+/+}$ and *H2AX*$^{-/-}$ spermatocytes was used to generate Cy5- or Cy3-labeled cDNA with the FairPlay Microarray Labeling Kit (Stratagene). Generated cDNAs were use to hybridize microarrays developed in the NCI/CCR μArray Center (version Mm-FCRF-GEM2-v3p17) by standard procedures. Microarray scanning and data extraction were performed with GenePix 3.0 software (Axon Instruments). Final data analysis was done in the *mAdb* Web interface (http://nciarray.nci.nih.gov).

Quantitative RT-PCR

Forty nanograms of total RNA from *H2AX*$^{+/+}$ and *H2AX*$^{-/-}$ spermatocytes was used for RT-PCR analysis with SYBR Green RT-PCR reagents following the manufacturer's instructions (Applied Biosystems). RT-PCRs were performed in an ABIPrism 7900HT Sequence Detection System and analyzed with the manufacturer's software, SDS 2.0 (Applied Biosystems). The following primer sequences were used: PGK2-5′, 5′-GTTGTAAAGGCCACCTCCAA-3′; PGK2-3′, 5′-ACATACGGGCGTCTTGATTC-3′; Rbmy-5′, 5′-CAAGAAGAGACCACCATCCT-3′; Rbmy-3′, 5′-CTCCCAGAAGAACTCACATT-3′; Ube1y-5′, 5′-CATTTTGTGGAAGGAGTTTCC-3′, Ube1y-3′, 5′-TCACAGAATAGGTAGGAGAC-3′. β-actin normalization primers were purchased from Clontech.

Acknowledgments

We thank M.A. Handel for helpful suggestions during the initial stages of this study; J. Turner for extensive technical advice; S. Pagakis and M. Kruhlak for help with image analysis; M.A. Handel, M. Lichten, A. Lee, and D.S. Singer for critical comments on the manuscript; T. Ried for providing chromosome-painting probes; and S. Ganesen, J. Pehrson, R. Scully, C. Heyting, R. Benavente, P. Singh, D. Elliott, P. Moens, H.-J. Garchon, and W. Earnshaw for sharing antibodies.

Received: March 3, 2003
Revised: March 4, 2003
Published: April 7, 2003

References

Abraham, R.T. (2001). Cell cycle checkpoint signaling through the ATM and ATR kinases. Genes Dev. *15*, 2177–2196.

Ayoub, N., Richler, C., and Wahrman, J. (1997). Xist RNA is associated with the transcriptionally inactive XY body in mammalian male meiosis. Chromosoma *106*, 1–10.

Baarends, W.M., Hoogerbrugge, J.W., Roest, H.P., Ooms, M., Vreeburg, J., Hoeijmakers, J.H., and Grootegoed, J.A. (1999). Histone ubiquitination and chromatin remodeling in mouse spermatogenesis. Dev. Biol. *207*, 322–333.

Bassing, C.H., Chua, K.F., Sekiguchi, J., Suh, H., Whitlow, S.R., Fleming, J.C., Monroe, B.C., Ciccone, D.N., Yan, C., Vlasakova, K., et al. (2002). Increased ionizing radiation sensitivity and genomic instability in the absence of histone H2AX. Proc. Natl. Acad. Sci. USA *99*, 8173–8178.

Baudat, F., Manova, K., Yuen, J.P., Jasin, M., and Keeney, S. (2000). Chromosome synapsis defects and sexually dimorphic meiotic progression in mice lacking Spo11. Mol. Cell *6*, 989–998.

Bauer, U.M., Schneider-Hirsch, S., Reinhardt, S., Benavente, R., and Maelicke, A. (1998). The murine nuclear orphan receptor GCNF is expressed in the XY body of primary spermatocytes. FEBS Lett. *439*, 208–214.

Burgoyne, P.S., Mahadevaiah, S.K., Sutcliffe, M.J., and Palmer, S.J. (1992a). Fertility in mice requires X-Y pairing and a Y-chromosomal "spermiogenesis" gene mapping to the long arm. Cell *71*, 391–398.

Burgoyne, P.S., Sutcliffe, M.J., and Mahadevaiah, S.K. (1992b). The role of unpaired sex chromosomes in spermatogenic failure. Andrologia *24*, 17–20.

Calenda, A., Allenet, B., Escalier, D., Bach, J.F., and Garchon, H.J. (1994). The meiosis-specific Xmr gene product is homologous to the lymphocyte Xlr protein and is a component of the XY body. EMBO J. *13*, 100–109.

Celeste, A., Petersen, S., Romanienko, P.J., Fernandez-Capetillo, O., Chen, H.T., Sedelnikova, O.A., Reina-San-Martin, B., Coppola, V., Meffre, E., Difilippantonio, M.J., et al. (2002). Genomic instability in mice lacking histone H2AX. Science *296*, 922–927.

Csankovszki, G., Panning, B., Bates, B., Pehrson, J.R., and Jaenisch, R. (1999). Conditional deletion of Xist disrupts histone macroH2A localization but not maintenance of X inactivation. Nat. Genet. *22*, 323–324.

Downs, J.A., Lowndes, N.F., and Jackson, S.P. (2000). A role for Saccharomyces cerevisiae histone H2A in DNA repair. Nature *408*, 1001–1004.

Drabent, B., Bode, C., Bramlage, B., and Doenecke, D. (1996). Expression of the mouse testicular histone gene H1t during spermatogenesis. Histochem. Cell Biol. *106*, 247–251.

Escalier, D., and Garchon, H.J. (2000). XMR is associated with the asynapsed segments of sex chromosomes in the XY body of mouse primary spermatocytes. Chromosoma *109*, 259–265.

Goetz, P., Chandley, A.C., and Speed, R.M. (1984). Morphological and temporal sequence of meiotic prophase development at puberty in the male mouse. J. Cell Sci. *65*, 249–263.

Hoyer-Fender, S., Costanzi, C., and Pehrson, J.R. (2000). Histone macroH2A1.2 is concentrated in the XY-body by the early pachytene stage of spermatogenesis. Exp. Cell Res. *258*, 254–260.

Jablonka, E., and Lamb, M.J. (1988). Meiotic pairing constraints and the activity of sex chromosomes. J. Theor. Biol. *133*, 23–36.

Keegan, K.S., Holtzman, D.A., Plug, A.W., Christenson, E.R., Brainerd, E.E., Flaggs, G., Bentley, N.J., Taylor, E.M., Meyn, M.S., Moss, S.B., et al. (1996). The Atr and Atm protein kinases associate with different sites along meiotically pairing chromosomes. Genes Dev. *10*, 2423–2437.

Keeney, S. (2001). Mechanism and control of meiotic recombination initiation. Curr. Top. Dev. Biol. *52*, 1–53.

Kralewski, M., Novello, A., and Benavente, R. (1997). A novel Mr 77,000 protein of the XY body of mammalian spermatocytes: its localization in normal animals and in Searle's translocation carriers. Chromosoma *106*, 160–167.

Lenhossek, M. (1898). Untersuchungen uber spermatogenese. Arch. Mikrosk. Anat. Entwicklungsmech *51*, 215–318.

Liyanage, M., Coleman, A., du Manoir, S., Veldman, T., McCormack, S., Dickson, R.B., Barlow, C., Wynshaw-Boris, A., Janz, S., Wienberg, J., et al. (1996). Multicolour spectral karyotyping of mouse chromosomes. Nat. Genet. *14*, 312–315.

Mahadevaiah, S.K., Odorisio, T., Elliott, D.J., Rattigan, A., Szot, M., Laval, S.H., Washburn, L.L., McCarrey, J.R., Cattanach, B.M., Lovell-Badge, R., and Burgoyne, P.S. (1998). Mouse homologues of the human AZF candidate gene RBM are expressed in spermatogonia and spermatids and map to a Y chromosome deletion interval associated with a high incidence of sperm abnormalities. Hum. Mol. Genet. *7*, 715–727.

Mahadevaiah, S.K., Turner, J.M., Baudat, F., Rogakou, E.P., de Boer, P., Blanco-Rodriguez, J., Jasin, M., Keeney, S., Bonner, W.M., and Burgoyne, P.S. (2001). Recombinational DNA double-strand breaks in mice precede synapsis. Nat. Genet. *27*, 271–276.

Manova, K., Tomihara-Newberger, C., Wang, S., Godelman, A., Kalantry, S., Witty-Blease, K., De Leon, V., Chen, W.S., Lacy, E., and Bachvarova, R.F. (1998). Apoptosis in mouse embryos: elevated levels in pregastrulae and in the distal anterior region of gastrulae of normal and mutant mice. Dev. Dyn. *213*, 293–308.

Mazeyrat, S., Saut, N., Grigoriev, V., Mahadevaiah, S.K., Ojarikre, O.A., Rattigan, A., Bishop, C., Eicher, E.M., Mitchell, M.J., and Burgoyne, P.S. (2001). A Y-encoded subunit of the translation initiation factor Eif2 is essential for mouse spermatogenesis. Nat. Genet. *29*, 49–53.

McCarrey, J.R., and Dilworth, D.D. (1992). Expression of Xist in mouse germ cells correlates with X-chromosome inactivation. Nat. Genet. *2*, 200–203.

McCarrey, J.R., Watson, C., Atencio, J., Ostermeier, G.C., Marahrens, Y., Jaenisch, R., and Krawetz, S.A. (2002). X-chromosome inactivation during spermatogenesis is regulated by an Xist/Tsix-independent mechanism in the mouse. Genesis *34*, 257–266.

McKee, B.D., and Handel, M. (1993). Sex chromosomes, recombination, and chromatin conformation. Chromosoma *102*, 71–80.

Miklos, G.L. (1974). Sex-chromosome pairing and male fertility. Cytogenet. Cell Genet. *13*, 558–577.

Moens, P.B., Chen, D.J., Shen, Z., Kolas, N., Tarsounas, M., Heng, H.H., and Spyropoulos, B. (1997). Rad51 immunocytology in rat and mouse spermatocytes and oocytes. Chromosoma *106*, 207–215.

Moens, P.B., Tarsounas, M., Morita, T., Habu, T., Rottinghaus, S.T., Freire, R., Jackson, S.P., Barlow, C., and Wynshaw-Boris, A. (1999). The association of ATR protein with mouse meiotic chromosome cores. Chromosoma *108*, 95–102.

Monesi, V. (1965). Synthetic activities during spermatogenesis in the mouse RNA and protein. Exp. Cell Res. *39*, 197–224.

Motzkus, D., Singh, P.B., and Hoyer-Fender, S. (1999). M31, a murine homolog of Drosophila HP1, is concentrated in the XY body during spermatogenesis. Cytogenet. Cell Genet. *86*, 83–88.

Nebel, B.R., Amarose, A.P., and Hackett, E.M. (1961). Calender of gametogenic development in the prepubertal male mouse. Science *134*, 832–833.

O'Carroll, D., Scherthan, H., Peters, A.H., Opravil, S., Haynes, A.R., Laible, G., Rea, S., Schmid, M., Lebersorger, A., Jerratsch, M., et al. (2000). Isolation and characterization of Suv39h2, a second histone H3 methyltransferase gene that displays testis-specific expression. Mol. Cell. Biol. *20*, 9423–9433.

Odartchenko, N., and Pavillard, M. (1970). Late DNA replication in male mouse meiotic chromosomes. Science *167*, 1133–1134.

Odorisio, T., Mahadevaiah, S.K., McCarrey, J.R., and Burgoyne, P.S. (1996). Transcriptional analysis of the candidate spermatogenesis gene Ube1y and of the closely related Ube1x shows that they are coexpressed in spermatogonia and spermatids but are repressed in pachytene spermatocytes. Dev. Biol. *180*, 336–343.

Odorisio, T., Rodriguez, T.A., Evans, E.P., Clarke, A.R., and Burgoyne, P.S. (1998). The meiotic checkpoint monitoring synapsis eliminates spermatocytes via p53-independent apoptosis. Nat. Genet. *18*, 257–261.

Painter, T.S. (1924). Studies in mammalian spermatogenesis III. The fate of the chromatin-nucleolus in the opossum. J. Exp. Zool. *39*, 197.

Parraga, M., and del Mazo, J. (2000). XYbp, a novel RING-finger protein, is a component of the XY body of spermatocytes and centrosomes. Mech. Dev. *90*, 95–101.

Perry, J., Palmer, S., Gabriel, A., and Ashworth, A. (2001). A short pseudoautosomal region in laboratory mice. Genome Res. *11*, 1826–1832.

Pittman, D.L., Cobb, J., Schimenti, K.J., Wilson, L.A., Cooper, D.M., Brignull, E., Handel, M.A., and Schimenti, J.C. (1998). Meiotic prophase arrest with failure of chromosome synapsis in mice deficient for Dmc1, a germline-specific RecA homolog. Mol. Cell *1*, 697–705.

Prophet, E.B. (1994). Laboratory Methods in Histotechnology, Third Edition (Washington, D.C.; American Registry of Pathology).

Raman, R., and Das, P. (1991). Mammalian sex chromosomes. III. Activity of pseudoautosomal steroid sulfatase enzyme during spermatogenesis in Mus musculus. Somat. Cell Mol. Genet. *17*, 429–433.

Rappold, G.A. (1993). The pseudoautosomal regions of the human sex chromosomes. Hum. Genet. *92*, 315–324.

Redon, C., Pilch, D., Rogakou, E., Sedelnikova, O., Newrock, K., and Bonner, W. (2002). Histone H2A variants H2AX and H2AZ. Curr. Opin. Genet. Dev. *12*, 162–169.

Richler, C., Ast, G., Goitein, R., Wahrman, J., Sperling, R., and Sperling, J. (1994). Splicing components are excluded from the transcriptionally inactive XY body in male meiotic nuclei. Mol. Biol. Cell *5*, 1341–1352.

Richler, C., Dhara, S.K., and Wahrman, J. (2000). Histone macroH2A1.2 is concentrated in the XY compartment of mammalian male meiotic nuclei. Cytogenet. Cell Genet. *89*, 118–120.

Roeder, G.S., and Bailis, J.M. (2000). The pachytene checkpoint. Trends Genet. *16*, 395–403.

Romanienko, P.J., and Camerini-Otero, R.D. (2000). The mouse Spo11 gene is required for meiotic chromosome synapsis. Mol. Cell *6*, 975–987.

Scully, R., Chen, J., Plug, A., Xiao, Y., Weaver, D., Feunteun, J., Ashley, T., and Livingston, D.M. (1997). Association of BRCA1 with Rad51 in mitotic and meiotic cells. Cell *88*, 265–275.

Singer-Sam, J., Robinson, M.O., Bellve, A.R., Simon, M.I., and Riggs, A.D. (1990). Measurement by quantitative PCR of changes in HPRT, PGK-1, PGK-2, APRT, MTase, and Zfy gene transcripts during mouse spermatogenesis. Nucleic Acids Res. *18*, 1255–1259.

Smith, A., and Benavente, R. (1992). Meiosis-specific protein selectively associated with sex chromosomes of rat pachytene spermatocytes. Proc. Natl. Acad. Sci. USA *89*, 6938–6942.

Smith, A., and Benavente, R. (1995). An Mr 51,000 protein of mammalian spermatogenic cells that is common to the whole XY body and centromeric heterochromatin of autosomes. Chromosoma *103*, 591–596.

Solari, A. (1974). The behavior of the XY pair in mammals. Int. Rev. Cytol. *38*, 273–317.

Strahl, B.D., and Allis, C.D. (2000). The language of covalent histone modifications. Nature *403*, 41–45.

Turner, J.M., Burgoyne, P.S., and Singh, P.B. (2001). M31 and macroH2A1.2 colocalise at the pseudoautosomal region during mouse meiosis. J. Cell Sci. *114*, 3367–3375.

Turner, J.M., Mahadevaiah, S.K., Benavente, R., Offenberg, H.H., Heyting, C., and Burgoyne, P.S. (2000). Analysis of male meiotic "sex body" proteins during XY female meiosis provides new insights into their functions. Chromosoma *109*, 426–432.

Turner, J.M., Mahadevaiah, S.K., Elliott, D.J., Garchon, H.J., Pehrson, J.R., Jaenisch, R., and Burgoyne, P.S. (2002). Meiotic sex chromosome inactivation in male mice with targeted disruptions of Xist. J. Cell Sci. *115*, 4097–4105.

Turner, J.M.A. (2000). An investigation into the role of sex chromosome synapsis in meiotic sex chromosome inactivation and fertility. PhD thesis, University College, London.

van Gent, D.C., Hoeijmakers, J.H., and Kanaar, R. (2001). Chromosomal stability and the DNA double-stranded break connection. Nat. Rev. Genet. *2*, 196–206.

Ward, I.M., and Chen, J. (2001). Histone H2AX is phosphorylated in an ATR-dependent manner in response to replicational stress. J. Biol. Chem. *276*, 47759–47762.

Wiltshire, T., Park, C., and Handel, M.A. (1998). Chromatin configuration during meiosis I prophase of spermatogenesis. Mol. Reprod. Dev. *49*, 70–80.

Yoshida, K., Kondoh, G., Matsuda, Y., Habu, T., Nishimune, Y., and Morita, T. (1998). The mouse RecA-like gene *Dmc1* is required for homologous chromosome synapsis during meiosis. Mol. Cell *1*, 707–718.